

# Optical Gain Performance of Epitaxially Grown *para*-Sexiphenyl Films\*\*

By Fabrizio Cordella,\* Francesco Quochi, Michele Saba, Andrei Andreev, Helmut Sitter, Niyazi Serdar Sariciftci, Andrea Mura, and Giovanni Bongiovanni

The great progress in the growth of ordered thin films of small linear molecules achieved in the past decade has made control of supramolecular arrangement and its effect on the physical properties frontline challenges for materials science. During film growth, multiple nucleation results in small, randomly oriented crystal domains. It has been recently shown that dipole-assisted, heteroepitaxial techniques allow deposition of thin films with unusual long-range order, consisting of crystalline aggregates that self-assemble to form nanofibers with sub-micrometer cross section, lengths of up to millimeters, orientational alignment extending to the centimeter size range, and controllable interaggregate distance.<sup>[1–3]</sup> These nanofibers have shown remarkable optical functionalities: photo- and electroluminescence,<sup>[2,4]</sup> optical waveguiding,<sup>[5,6]</sup> frequency doubling,<sup>[7]</sup> and optical gain.<sup>[8,9]</sup> Very recently, we have also shown that, depending on the growth condition, a single nanofiber behaves as a low-threshold self-assembled laser resonator, with randomly distributed optical feedback provided by 100 nm wide fiber breaks.<sup>[10]</sup> The high sensitivity of laser action to (bio)chemical contamination has been recently used to demonstrate nonlinear optical sensors with superior sensitivity.<sup>[11]</sup> For this purpose, nanofiber lasers offer several

advantages: easy fabrication, a very favorable surface-to-volume ratio that may result in a more facile achievement of high concentrations of contaminants, the potential of molecular functionalization<sup>[12]</sup> for selective sensitizing, and finally, multi-target and multichannel detection, thanks to the possibility of using an ensemble of nanoresonators, each one with a specific functionalization and oscillation frequency pattern.<sup>[10]</sup> Furthermore, a single nanofiber or ensemble of nanofibers can, after heteroepitaxial growth, be transferred onto suitable substrates, or in a liquid environment, for a specific application.<sup>[13]</sup>

Lasing performance results from extrinsic factors (e.g., optical feedback and losses) and from the intrinsic gain response of the active material. This latter depends on both the properties of the single molecule and the strength of intermolecular interactions, and thus on the degree of supramolecular order. The potential of a material to amplify light can be quantified in terms of a few basic parameters: the gain bandwidth ( $\Gamma_g$ ) over which light amplification can occur, which ultimately determines the lasing tunability, and the optical amplification rate under cw excitation; this latter quantity scales as the gain cross section times the gain lifetime ( $\sigma_g \tau_g$ ), which, balancing optical losses, contributes to determining the lasing threshold.

Organic lasers always try to get the best out of two worlds, by combining the large gain bandwidth of isolated molecules with the high concentration of molecules achievable in the solid state. However, recent research clearly indicates that intermolecular interactions in the solid state can quench the optical gain.<sup>[14]</sup> Typical critical issues are the appearance of additional photoinduced absorption (PA) bands and nonradiative decay channels, which reduce the size of the optical gain overall, narrow its effective spectral width, and shorten the gain lifetime. In the class of linear oligomers, PA bands arise on the low-energy side of the gain spectrum from singlet, triplet, and polaron states, whereas long-lived polaron pairs yield additional PA bands close to the optical gap energy ( $E_g$ ).<sup>[14,15]</sup> Such phenomena are not easily predicted from molecular properties or photoluminescence spectra, and typically need nonlinear spectroscopy techniques to be fully characterized. Most experimental studies on long-lived polaron pairs concern the family of phenylenevinylene oligomers and polymers,<sup>[14–19]</sup> while much less information is available on phenylenes, which represent a very important class of  $\pi$ -conjugated molecules for light amplification.<sup>[20–22]</sup>

In this Communication, we explore the basic gain performance of a model molecular system used to grow organic het-

[\*] Dr. F. Cordella, Dr. F. Quochi, Dr. M. Saba, Prof. A. Mura, Prof. G. Bongiovanni  
Dipartimento di Fisica, Università degli Studi di Cagliari  
09042 Monserrato (Italy)  
E-mail: fabrizio.cordella@dsf.unica.it

Dr. A. Andreev  
Institute of Physics, University of Leoben  
8700 Leoben (Austria)

Prof. H. Sitter  
Institute of Semiconductors and Solid State Physics  
Johannes Kepler University Linz  
4040 Linz (Austria)

Prof. N. S. Sariciftci  
Linz Institute for Organic Solar Cells (LIOS) Physical Chemistry  
Johannes Kepler University Linz  
4040 Linz (Austria)

[\*\*] The authors thankfully acknowledge fruitful discussions with F. Balzer and H. G. Rubahn. The work in Cagliari has been partially funded by MIUR through FIRB projects (Synergy-FIRBRBNE03S7XZ and FIRB-RBAU01N449), by the European commission through the Human Potential Programs (RTN Nanomatch, Contract No. MRTN-CT-2006-035884). M.S. acknowledges the Italian Government Program 'Rientro dei Cervelli'. The work in Linz is supported by the Austrian Science Foundation (Projects No. NFN S9706, NFN S9707, and NFN S9711).

eroepitaxial films: *para*-sexiphenyl (*p*-6P).<sup>[1–3]</sup> The excited-state dynamics is studied using time-resolved pump-probe spectroscopy, namely, we look at the effects induced by pump pulses on the energy of probe pulses transmitted at various time delays ( $\Delta t$ ) through a *p*-6P film. To extend the investigation of the photophysical properties from the mid-gap to the optical gap ( $E_g = 3.06$  eV), we have developed a pump-probe technique with probe photon energies up to the deep blue (3.15 eV), yielding differential transmission ( $\Delta T/T$ ) spectra with root mean square sensitivity down to ca.  $10^{-4}$  (see Experimental). The excited-state dynamics is reconstructed from the time evolution of the  $\Delta T/T$  spectrum, which exhibits both stimulated emission (SE) from singlet excitons and PA from species identified as triplet excitons, polarons, and correlated polaron pairs. We demonstrate how the combination of high structural order and low lattice temperature leads to an unmatched gain spectral width, with a lifetime in the nanosecond time domain for cw lasing applications in organic molecular nanoaggregates.

A typical microscopy image of a *p*-6P film on a mica substrate featuring highly oriented needles is shown in the inset of Figure 1a. The long axis of the *p*-6P molecules and the optical dipole of the lowest optical transition are nearly parallel to the sample surface and perpendicular to the needle direction. This molecular geometry enables us to probe optical gain with polarization parallel to the oligomers axis.

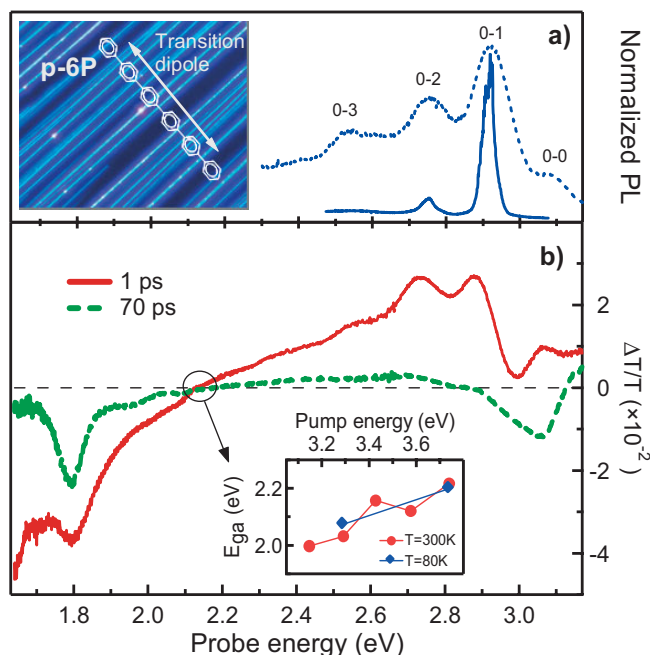


**Figure 1.** a) cw-spontaneous emission (dotted curve) and amplified spontaneous emission (continuous curve) spectrum at  $T = 300$  K. Inset: fluorescence image of a  $140 \times 110 \mu\text{m}^2$  region of an epitaxially grown *p*-6P thin film featuring sparse needles. b) Differential transmission ( $\Delta T/T$ ) spectra taken at  $T = 300$  K for various pump-probe delays; excitation energy fluence:  $\Phi_{\text{ex}} = 90 \mu\text{J cm}^{-2}$  per pulse; pump photon energy:  $h\nu_p = 3.44$  eV. Polarization of the probe beam is parallel to the molecular axis. Inset: gain-to-absorption crossover energy (isosbestic point) measured at zero delay versus pump photon energy.

Figure 1a shows the photoluminescence spectrum of *p*-6P nanofibers at room temperature. The emission spectrum shows the typical features of H aggregates,<sup>[23,24]</sup> that is, a weak electronic (0–0) transition and a more intense vibronic progression involving the C–C stretching mode. As recently shown, pump fluences ( $\Phi_{\text{ex}}$ ) as low as  $1\text{--}10 \mu\text{J cm}^{-2}$  (per pulse) yield efficient amplification of light propagating along the nanofibers.<sup>[8]</sup> Depending on the amount of optical feedback provided by randomly distributed needle breaks, single-fiber lasing or amplification of spontaneous emission (ASE) are observed.<sup>[9,10]</sup> A typical example of the latter is reported in Figure 1. ASE and laser action always start at the 0–1 band and then extend to the 0–2 vibronic replica at higher excitation intensities. Figure 1b shows differential transmission spectra ( $\Delta T/T$ ) for  $\Phi_{\text{ex}} = 90 \mu\text{J cm}^{-2}$ , pump photon energy equal to 3.44 eV, and pump polarization parallel to the *p*-6P long axis. The films used in the experiments were selected so as to exhibit high lasing threshold fluences; the rate of light amplification was thus low enough not to perturb the excited-state dynamics. At  $\Delta t = 1$  ps, the pump pulses induce an increase of the probe transmission ( $\Delta T/T > 0$ ) over a wide spectral range, which extends from the deep blue to the orange, that is, down to ca. 1 eV below  $E_g$ . The positive  $\Delta T/T$  signal can be attributed to stimulated optical transitions from the singlet state  $S_1$  to up the fifth C–C vibrational level of the ground state and to bleaching of the 0–0 electronic transition. This very large, molecularlike, gain bandwidth confirms the potential of epitaxially grown *p*-6P aggregates for light-amplification applications.

The low-energy onset of gain is determined by mid-gap excited-state absorption, specifically from triplet and unbound polaron states at 1.8 and 2.05 eV, respectively (see the discussion in the subsequent paragraph). These bands are characterized by a prompt response to the short pump pulses. The photon energy ( $E_{\text{ga}}$ ) at which gain-to-absorption cross over occurs (isosbestic point) slightly depends on the pump photon energy ( $h\nu_p$ );  $E_{\text{ga}}$  increases from 2.0 to 2.2 eV, for  $h\nu_p$  ranging from 3.05 to 3.8 eV (see inset of Fig. 1b). On the other hand,  $E_{\text{ga}}$ , and thus the effective gain bandwidth  $\Gamma_g$ , is strongly dependent on the interaction with the substrate. Films deposited on more conventional substrates, like quartz plates, have a smaller gain bandwidth ( $\Gamma_g \sim 0.5$  eV),<sup>[25,26]</sup> which is half the one observed in heteroepitaxial films grown on mica. Near-gap PA is observed at longer delays. At  $\Delta t = 70$  ps, a new PA band is visible close to the 0–0 transition, partially overlapping with the 0–1 peak of the (decayed) SE band.

The temporal evolution of the  $\Delta T/T$  spectrum near  $E_g$  is displayed in detail in Figure 2. The activation dynamics of the near-gap PA signal is rather complex, showing an initial fast transient peak at 2.98 eV and a slower component that ends up with a band at 3.06 eV; this latter exhibits a decay time longer than 1 ns. The rise time of such long-lived PA band (ca. 10 ps) is complementary to the short 10 ps initial decay of SE (see Fig. 2b), which suggests that new intermolecular species (polaron pairs, see the discussion in the following) are formed as a product of the singlet exciton recombination pro-

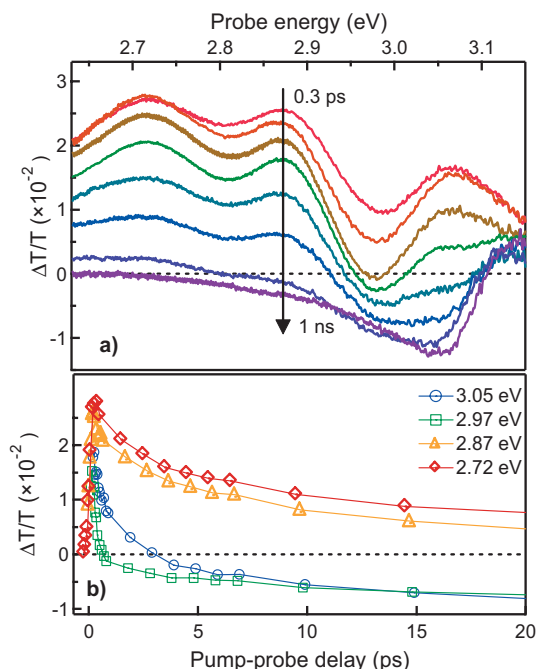


**Figure 2.** a)  $\Delta T/T$  spectra taken at  $T=300$  K for the pump-probe delays of 0.3, 0.5, 1, 2, 5, 15, 75 ps, and 1 ns; excitation energy fluence  $\Phi_{\text{ex}}=90 \mu\text{J cm}^{-2}$  per pulse; pump photon energy:  $h\nu_p=3.44$  eV. b)  $\Delta T/T$  time traces generated for different probe photon energies with the same experimental conditions as in (a).

cess. In the excitation regime used in the experiment, singlet exciton recombination is mainly a bimolecular process<sup>[15]</sup> that results in a doubly negative impact on the gain response, shortening the SE lifetime  $\tau_g$  and shrinking the SE bandwidth through the activation of polaron pairs responsible for near-gap PA; the former effect is especially detrimental to achieving laser action under cw pumping.

To reduce the impairing effect of bimolecular recombination on the gain performance, we first extended room-temperature  $\Delta T/T$  measurements to decreasing values of the pump fluence. Figure 3a shows  $\Delta T/T$  transients at the photon energies of the 0–2 and 0–0 transition peaks to monitor the decay of singlet excitons and the activation of the high-energy polaron pairs, respectively. For decreasing  $\Phi_{\text{ex}}$  from 75 to 20  $\mu\text{J cm}^{-2}$ , the initial singlet recombination rate constant slows down, as expected to occur in the bimolecular regime, although remaining still much faster than the monomolecular decay constant ( $1/500 \text{ ps}^{-1}$  as determined from time-resolved photoluminescence data recorded at much lower pump fluences). Lowering the pump fluence down to some 20  $\mu\text{J cm}^{-2}$  results in a slower, though still detectable, formation of polaron pairs (time trace marked with empty dots in Fig. 3a).

An alternate route to suppress bimolecular recombination is the reduction of exciton diffusion, and hence exciton–exciton reactions, which can be achieved by lowering the lattice temperature.<sup>[27]</sup>  $\Delta T/T$  transients at  $T=80$  K for the same pump fluences used at room temperature (shown in Fig. 3b) demonstrate that decreasing the temperature strongly sup-

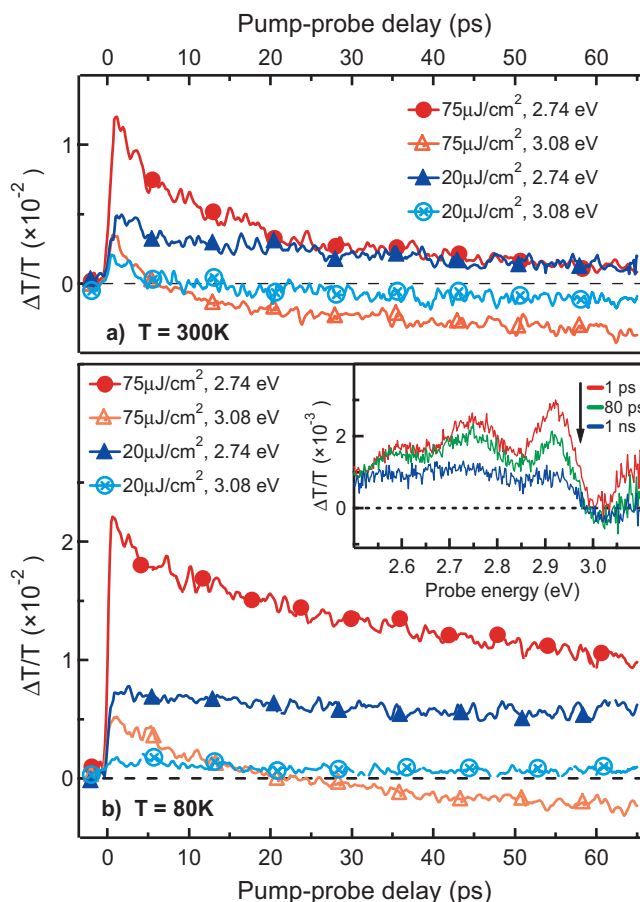


**Figure 3.**  $\Delta T/T$  time traces taken for different pump fluences and probe photon energies at  $T=300$  (a) and 80 K (b); pump photon energy:  $h\nu_p=3.54$  eV. Inset of panel (b) Near-gap  $\Delta T/T$  spectra measured for  $\Phi_{\text{ex}}$  ca.  $10 \mu\text{J cm}^{-2}$ .

presses singlet–singlet annihilation. The inset of Figure 3b shows a series of  $\Delta T/T$  spectra at different delays for  $\Phi_{\text{ex}}$  ca.  $10 \mu\text{J cm}^{-2}$ , an excitation regime low enough that the activation of the near-gap PA band becomes negligible and the gain lifetime (ca. 1 ns) matches the low-temperature photoluminescence lifetime.

The gain bandwidth in organic nanofibers is limited by two distinct photophysical processes, one generating PA at the low-energy end of the gain spectrum, the other one on the high-energy side. The PA limiting the gain bandwidth at low energies in *p*-6P has been attributed to the disorder-induced formation of polarons and triplet excitons.<sup>[26]</sup> Such a conclusion supports the speculation that the much larger extent of gain bandwidth at low energies observed in our epitaxial samples on mica is due to the minimization of structural disorder, leading to the inhibition of polaron and triplet-state creation through extrinsic processes. Intrinsic mechanisms for polaron formation can be possibly activated by increasing the photon excess energy  $\Delta E_g$ , which would explain the blue shift observed in the (low-energy) isosbestic point shown in the inset of Figure 1b.<sup>[28]</sup>

The PA high-energy band that limits the gain near the optical bandgap energy  $E_g$  does not appear instantaneously after pump excitation and seems instead to have more of an intrinsic origin. Such a PA band has also been reported in oligophenylenevinylene films<sup>[14–16]</sup> and attributed to Coulomb-correlated polaron pairs (intermolecular excitons), which are generated as a by-product of the exciton bimolecular process. The proposed reaction scheme was the following: in the singlet–singlet annihilation event, the energy of one exciton is transferred to the second interacting exciton, which is consequently promoted to a hot level. The energy of this neutral state (ca. 6 eV) is high enough to undergo autoionization, resulting in the generation of a pair of oppositely charged polarons. Under an applied electric field, these neutral excitations could be split into unbound carriers to yield photocurrent, as demonstrated in tetracene crystals decades ago.<sup>[29]</sup>

This limitation to the gain spectrum at high energy is particularly cumbersome, as it becomes more and more important at high excitation densities and is nearly resonant with optical emission, therefore representing the most effective channel of gain quenching and conflicting with the need of inverting the optical transition in a laser medium. However, our low-temperature measurements demonstrate a regime where singlet–singlet recombination is suppressed and, consequently, the gain lifetime reaches in the nanosecond time scale already at pump fluences high enough (ca.  $10 \mu\text{J cm}^{-2}$ ) to initiate laser action in low-loss *p*-6P nanofiber films. From these results one infers that lasing thresholds in the  $1\text{--}10 \mu\text{J cm}^{-2}$  range under femtosecond pulse excitation correspond to thresholds of  $1\text{--}10 \text{ kW cm}^{-2}$  under continuous-wave or nanosecond-long pulse (quasi-steady-state) excitation regime.

The SE cross section ( $\sigma_g$ ) of *p*-6P in our heteroepitaxial films is found to be ca.  $2 \times 10^{-16} \text{ cm}^2$ ,<sup>[30]</sup> as estimated from the  $\Delta T/T$  signal amplitude (at  $\Delta t = 0$ ) at the 0–2 vibronic peak with the assumption that mainly singlet excitons are photogenerated by the pump pulses. The size of  $\sigma_g$  is comparable to the estimates reported in most works on thin films of conjugated oligomers; moreover, it is worth mentioning that in solution these molecules should display even larger  $\sigma_g$  values (of some  $10^{-15} \text{ cm}^2$ ), as can be deduced from the emission lifetime and quantum yield through the Strickler–Berg law.<sup>[31]</sup> According to the theory developed by Spano for H aggregates,<sup>[23]</sup> smaller values of  $\sigma_g$  in the solid state are realized as a consequence of resonant intermolecular interactions, which lower the effective oscillator strength of the vibronic transitions.

The understanding of the photophysical processes involved in optical gain performance in *p*-6P suggests new avenues to go around limitations and design advanced crystalline materials with improved light amplification properties. One strategy could be doping *p*-6P crystals with linear molecules emitting at lower energies. This approach can bring to the table several advantages: i) excitations would be funneled via Förster energy transfer from the *p*-6P matrix to the emitting acceptors, where they would be immobilized, thus contrasting efficiently bimolecular reactions; ii) owing to the large exciton diffusion

coefficient in ordered molecular crystals, acceptor concentrations as low as 0.1–1 % should be enough to guarantee energy transfer; iii) The SE cross section of dopant molecules should not be reduced by resonant (H-type) intermolecular interaction, while iv) residual excitations in the *p*-6P matrix would still provide the material system with an extra, 1 eV wide gain bandwidth for further applications. The doping approach resembles to some extent the one used, almost twenty years ago, to achieve lasing in fluorene crystals doped with anthracene,<sup>[32]</sup> or the one used to reduce lasing threshold in amorphous molecular films.<sup>[33]</sup> In addition, ordered molecular matrices should also benefit from improved charge-transport properties.<sup>[34]</sup>

We have shown that the gain bandwidth of *p*-6P nanofibers grown by heteroepitaxial techniques spans the visible range for ca. 1 eV, thanks to the reduced contribution of mid-gap photoabsorption. Tuning pump photon energy across the lowest  $\pi\text{--}\pi^*$  Davydov band has minor effects on the gain spectrum. Exciton–exciton annihilation processes drastically shorten the gain lifetime  $\tau_g$  and lead to a near-gap PA band, in the deep blue, which is related to the formation of long-lived polaron pairs. By lowering the temperature, bimolecular exciton recombination is suppressed; the formation of polaron pairs is thus inhibited and a 1 ns long gain lifetime is recovered, which is promising for laser applications in the cw or quasi-steady-state regime. Finally, the present results suggest that ordered molecular aggregates doped with low-energy emitting molecules could result in organic materials systems with improved optical gain performance, still preserving optimal charge-transport properties.

## Experimental

*Para*-sexiphenyl (*p*-6P) was purified by threefold sublimation under dynamic vacuum, then grown by hot-wall epitaxy [2] on freshly cleaved (001)-oriented muscovite mica. The base pressure during growth was ca.  $6 \times 10^{-6}$  mbar (1 bar = 100 000 Pa) and the *p*-6P source temperature was fixed at 240 °C. The substrate temperature was 130 °C. The growth time was varied from 10 s to 120 min to obtain samples ranging from thin films with sparse needles to thick (ca. 400 nm) films with highly packed needles. Pump-probe spectroscopy was performed on a 300 nm thick film. The sample was pumped by a 1 kHz train of ca. 100 fs long pulses delivered by either one of two tunable optical parametric amplifiers (Light Conversion Topas and Topas White) or by the second harmonic of a Ti:Sa amplified laser (Quantronix Integra, 1.5 mJ output energy). To measure the  $\Delta T/T$  spectrum, the sample was probed by a white (supercontinuum) laser beam. A white probe beam ranging between 1.7 and 2.7 eV in photon energy was generated focusing the output (at 1.58 eV) of the Ti:Sa laser onto a 4 mm thick sapphire plate; a supplementary broadband probe beam extending from 2.7 to 3.15 eV was in turn produced using the output (at 2.23 eV) of either one of the two parametric amplifiers. Pump-probe time delay was controlled using a motorized optical delay stage. Balanced detection was used [35] to obtain  $\Delta T/T$  sensitivities down to about  $10^{-4}$  (root mean square) in the probe energy range from 1.7 to 3.15 eV, using integration times of ca. 1–2 min. The chirp of the white probe was corrected by software, which yielded nearly dispersion-free spectrograms across the entire probe energy range used in the experiments.  $\Delta T/T$  time traces at given probe photon ener-

gies were taken using the output beams of the two parametric amplifiers as the pump and the probe. Low-temperature measurements were made using a low-vibration, LN<sub>2</sub>-cooled cold-finger cryostat.

Received: March 15, 2007  
Published online: July 27, 2007

- [1] T. Mikami, H. Yanagi, *Appl. Phys. Lett.* **1998**, *73*, 563.
- [2] A. Andreev, G. Matt, C. J. Brabec, H. Sitter, D. Badt, H. Seyringer, N. S. Sariciftci, *Adv. Mater.* **2000**, *12*, 629.
- [3] F. Balzer, H.-G. Rubahn, *Nano Lett.* **2002**, *2*, 747.
- [4] H. Yanagi, T. Morikawa, S. Hotta, *Appl. Phys. Lett.* **2002**, *81*, 1512.
- [5] H. Yanagi, T. Morikawa, *Appl. Phys. Lett.* **1999**, *75*, 187.
- [6] F. Balzer, V. G. Bordo, A. C. Simonsen, H.-G. Rubahn, *Appl. Phys. Lett.* **2003**, *82*, 10.
- [7] J. Brewer, M. Schiek, A. Lützen, K. Al-Shamery, H.-G. Rubahn, *Nano Lett.* **2007**, *6*, 2656.
- [8] F. Quochi, F. Cordella, R. Orrù, J. E. Communal, P. Verzeroli, A. Mura, G. Bongiovanni, A. Andrees, H. Sitter, N. S. Sariciftci, *Appl. Phys. Lett.* **2004**, *84*, 4454.
- [9] F. Quochi, F. Cordella, A. Mura, G. Bongiovanni, F. Balzer, H.-G. Rubahn, *Appl. Phys. Lett.* **2006**, *88*, 41 106.
- [10] F. Quochi, F. Cordella, A. Mura, G. Bongiovanni, F. Balzer, H.-G. Rubahn, *J. Phys. Chem. B* **2005**, *109*, 21 690.
- [11] A. Rose, Z. Zhu, C. F. Madigan, T. M. Swager, V. Bulovic, *Nature* **2005**, *434*, 876.
- [12] M. Schiek, A. Lützen, K. Al-Shamery, F. Balzer, H.-G. Rubahn, *Cryst. Growth Des.* **2007**, *7*, 229.
- [13] F. Balzer, H.-G. Rubahn, *Adv. Funct. Mater.* **2005**, *15*, 17.
- [14] N. S. Sariciftci, *Primary Photoexcitations in Conjugated Polymers*, World Scientific, Singapore **1997**.
- [15] M. Pope, C. E. Swenberg, *Electronic Processes in Organic Crystals and Polymers*, Oxford University Press, New York **1999**.
- [16] C. Cerullo, G. Lanzani, S. De Silvestri, H.-J. Egelhaaf, L. Lüer, D. Oelkrug, *Phys. Rev. B* **2000**, *62*, 2429.
- [17] S. V. Frolov, Z. Bao, M. Wolgenannt, Z. V. Vardeny, *Phys. Rev. B* **2002**, *65*, 205 209.
- [18] a) M. Yan, L. J. Rothberg, F. Papadimitrakopoulos, M. E. Galvin, T. M. Miller, *Phys. Rev. Lett.* **1994**, *72*, 1104. b) M. Yan, L. J. Rothberg, E. W. Kwock, T. M. Miller, *Phys. Rev. Lett.* **1995**, *75*, 1992.
- [19] A. Köhler, D. A. dos Santos, D. Beljonne, Z. Shuai, J.-L. Brédas, A. B. Holmes, A. Kraus, K. Mullen, R. H. Friend, *Nature* **1998**, *392*, 903.
- [20] D. Fichou, S. Delysse, J.-M. Nunzi, *Adv. Mater.* **1997**, *9*, 1178.
- [21] M. Ichikawa, R. Hibino, M. Inoue, T. Haritani, S. Hotta, T. Koyama, Y. Taniguchi, *Adv. Mater.* **2003**, *15*, 213.
- [22] R. Hibino, M. Nagawa, S. Hotta, M. Ichikawa, T. Koyama, Y. Taniguchi, *Adv. Mater.* **2002**, *14*, 119.
- [23] F. C. Spano, *Annu. Rev. Phys. Chem.* **2006**, *57*, 217.
- [24] F. Meinardi, M. Cerminara, A. Sassella, A. Borghesi, P. Spearman, G. Bongiovanni, A. Mura, R. Tubino, *Phys. Rev. Lett.* **2002**, *89*, 157 413.
- [25] A. Piaggi, G. Lanzani, G. Bongiovanni, A. Mura, W. Graupner, F. Meghdadi, G. Leising, M. Nisoli, *Phys. Rev. B* **1997**, *56*, 10 133.
- [26] C. Zenz, G. Cerullo, G. Lanzani, W. Graupner, F. Meghdadi, G. Leising, S. De Silvestri, *Phys. Rev. B* **1999**, *59*, 14 336.
- [27] H. Weisenhofer, E. Zojer, E. J. W. List, U. Scherf, J.-L. Brédas, D. Beljonne, *Adv. Mater.* **2006**, *18*, 310.
- [28] L. Lüer, C. Manzoni, H.-J. Egelhaaf, G. Cerullo, D. Oelkrug, G. Lanzani, *Phys. Rev. B* **2006**, *73*, 035 216.
- [29] G. R. Johnston, L. E. Lyons, *Aust. J. Chem.* **1970**, *23*, 1571.
- [30] The present estimate of the SE cross section is about seven times smaller than that calculated from the size of the modal gain in single nanofiber, assuming an optical confinement of 1 %. Underestimation of the confinement factor, which may result from having neglected gain guiding effects, can explain the previous overestimation of the SE cross section [9].
- [31] S. J. Strickler, R. A. Berg, *J. Chem. Phys.* **1962**, *37*, 814.
- [32] a) N. Karl, *Phys. Status Solidi A* **1972**, *13*, 651. b) N. Karl, *J. Lumin.* **1976**, *12/13*, 851.
- [33] M. Berggren, A. Dodabalapur, R. E. Slusher, Z. Bao, *Nature* **1997**, *389*, 466.
- [34] a) B. Singh, G. Hernandez-Sosa, H. Neugebauer, A. Andreev, H. Sitter, N. S. Sariciftci, *Phys. Status Solidi B* **2006**, *243*, 3329. b) A. Montaigne Ramil, B. Singh, N. Haber, N. Marjanovic, S. Guenes, A. Andreev, G. Matt, R. Resel, H. Sitter, N. S. Sariciftci, *J. Cryst. Growth* **2006**, *288*, 123. c) A. Mozer, N. S. Sariciftci, *Chem. Phys. Lett.* **2004**, *389*, 438.
- [35] F. Cordella, R. Orru, M. A. Loi, A. Mura, G. Bongiovanni, *Phys. Rev. B* **2003**, *68*, 113 203.